

1 **Projected increases in wildfires may challenge regulatory curtailment of PM_{2.5} over the**
2 **eastern US by 2050**

3

4 Chandan Sarangi^{1,2*}, Yun Qian^{2*}, L. Ruby Leung², Yang Zhang³, Yufei Zou^{4,2}, Yuhang
5 Wang⁴

6

7 ¹ Indian Institute of Technology Madras, Chennai, India

8 ² Pacific Northwest National Laboratory, Richland, WA, USA

9 ³ Department of Civil and Environmental Engineering, Northeastern University, Boston, MA

10 ⁴ School of Earth and Atmospheric Sciences, Georgia Institute of Technology, Atlanta, GA,
11 USA.

12

13

14 *Corresponding Authors:

15 chandansarangi@iitm.ac.in

16 yun.qian@pnnl.gov

17

18

19

20

21 **Abstract**

22 Anthropogenic contribution to the overall fine particulate matter (PM_{2.5}) concentrations has
23 been declining sharply in North America. In contrast, a steep rise in wildfire-induced air
24 pollution events with recent warming is evident in the region. Here, based on coupled fire-
25 climate-ecosystem model simulations, summertime wildfire-induced PM_{2.5} concentrations are
26 projected to nearly double in North America by the mid-21st century compared to the
27 present. More strikingly, the projected enhancement in fire-induced PM_{2.5} (~ 1-2 µg/m³) and
28 its contribution (~15-20%) to the total PM_{2.5} are distinctively significant in the eastern US.
29 This can be attributed to downwind transport of smoke from future enhancement of wildfires
30 in North America to the eastern US and associated positive climatic feedback on PM_{2.5} i.e.
31 perturbations in circulation, atmospheric stability and precipitation. Therefore, the anticipated
32 reductions in PM_{2.5} from regulatory controls on anthropogenic emissions could be
33 significantly compromised in the future in the densely populated eastern US.

34 **Key points:**

- 35 1) Wildfire-PM_{2.5} associations studied based on unprecedented two-way coupled fire-
36 climate-ecosystem model simulations
- 37 2) A steep rise in wildfire-induced air pollution events with recent warming is evident in
38 the region
- 39 3) The transported smoke from enhanced wildfires in North America can severely affect
40 air quality over Eastern US

41

42 **Keywords:** wildfire emissions, climate change, air quality, smoke transport, wildfire-climate-
43 ecosystem interactions

44 **1. Introduction**

45 Wildfires are widespread burning events in forests, shrub lands, and grazing lands. In
46 North America (mainly Canada and the US), particulate matter emissions from wildfires are a
47 significant source of regional air pollution (Shi et al., 2019; McClure and Jaffe, 2018; Van
48 Der Werf et al., 2010; Jaffe et al., 2008). Since the 1980s, the number of large wildfires and
49 the length of wildfire season have been increasing, and the trends are projected to continue in
50 the future over the western US, Alaska and Canada (Kitzberger et al., 2017; Kirchmeier-
51 Young et al., 2017; Abatzoglou and Williams, 2016; Partain et al., 2016; Jolly et al., 2015;
52 Westerling et al., 2006; Gillett et al., 2004). Accordingly, particulate emissions from wildfires
53 are also anticipated to increase in North America in the 21st century (Knorr et al., 2017; Liu
54 et al., 2016; Val Martin et al., 2015). Human exposure to high concentrations of wildfire-
55 emitted airborne particulate matter of diameter $\leq 2.5 \mu\text{m}$ (PM_{2.5}) is known to have substantial
56 adverse effects on pulmonary and cardiovascular functioning (Anjali et al., 2019; Black et al.,
57 2017), which contribute significantly to global and regional all-cause mortality (Zhang et al.,
58 2020; Hong et al., 2019; Yang et al., 2019; Ford et al., 2018; Johnston. et al., 2012).
59 Therefore, a better understanding of the future changes in wildfire-induced PM_{2.5} and its
60 contribution to the total surface PM_{2.5} is essential.

61 In the last two decades, ambient air quality in the US has substantially improved due
62 to a decline in PM_{2.5} by ~ 40 % (US EPA, 2018). The decrease in PM_{2.5} is primarily due to
63 curtailment of anthropogenic emissions resulting from US-based efforts to meet regulations
64 such as the Clean Air Act (US EPA, 2009), Cross-State Air Pollution Rule, Regional Haze
65 Rule, and the motor vehicles emissions standards. Consequently, air quality over the
66 contiguous US (CONUS) and Canada has improved steadily such that it is predicted to
67 achieve the targeted National Ambient Air Quality Standards in the future (Nolte et al.,

68 2018). Under this promising scenario, the influence of wildfire-emissions on the total PM_{2.5}
69 becomes even more crucial. Depending on the competition between climate-induced increase
70 in wildfires and the regulatory control on anthropogenic emissions, future enhancement in
71 wildfire-induced PM_{2.5} may compromise the reduction in anthropogenic PM_{2.5} concentrations
72 in certain regions. In agreement, recent studies have highlighted the potential for future
73 enhancement in wildfire-induced pollution to diminish the reducing trend in PM_{2.5}, primarily
74 over the western US (O'Dell et al., 2019; Ford et al., 2018; Val Martin et al., 2015; Yue et al.,
75 2013).

76 While the fractional wildfire burnt area and fire intensities are the greatest over the
77 western US and Canadian regions within North America, anthropogenic emissions dominate
78 the ambient PM_{2.5} concentration over the eastern US. The inherent geographical separation
79 between the regions with large wildfire emissions and anthropogenic emissions leads to a
80 pertinent question: will future enhancement in wildfires over the western US and Canada
81 have significant effects on PM_{2.5} over the eastern US? Addressing this question is crucial
82 because the declining trend in PM_{2.5} over the eastern US is the major contributor to the
83 observed 40% decrease in PM_{2.5} over the US in the last two decades (US EPA, 2018).
84 Eastward advection of wildfire smoke from Canada and the western US has been found to
85 severely hamper the surface air quality of the central and eastern US under the influence of
86 the prevailing westerlies during the summer months (Brey et al., 2018; Wu et al., 2018;
87 Gunsch et al., 2018; Kaulfus et al., 2017; Dempsey, 2013). The transported wildfire smoke
88 can influence the meteorology and climate via the radiative impact of carbonaceous
89 emissions, changes in land albedo and cloud system perturbations (Ward et al., 2012; Liu et
90 al., 2014). These fire-weather interactions can have positive feedback on the locally-emitted
91 PM_{2.5} in the eastern US by surface cooling and boundary layer suppression (Guan et al.,
92 2020). At the same time, fire-triggered ecosystem changes can induce negative feedback on

93 PM_{2.5} by reducing the future wildfires over North America (Zou et al., 2020). Thus, two-
94 way interactions between fires and climate that are important for predicting future changes in
95 wildfire locations, intensities, and durations (Harris et al., 2016) as well as associated
96 particulate emissions is essential. However, past studies have mostly employed simple
97 statistical models based on statistical regressions of present-day fire burnt area on the
98 meteorological fields (Liu et al., 2016; Spracklen et al., 2009; Yue et al., 2013; Val Martin et
99 al., 2015), and more recently, one-way coupled modelling (Ford et al., 2018; O’Dell et al.,
100 2019).

101 Here, based on new two-way coupled fire-climate-ecosystem simulations, we
102 demonstrate the significance of wildfire-induced contributions to ambient PM_{2.5} over the
103 eastern US due to enhanced wildfire smoke transportation and smoke-induced changes in
104 weather in eastern US. This enhancement in wildfire-induced PM_{2.5} may potentially challenge
105 the targeted policy-driven reduction of PM_{2.5} in the eastern US. Next, our model setup,
106 experiments and methodology are explained in Section 2, followed by results and discussion
107 in Section 3. The study is summarized in Section 4.

108 **2. Materials and Methods**

109 **2.1. RESFire-CESM Model description**

110 We employ the open-source REgion-Specific ecosystem feedback fire (RESFire)
111 model coupled with the Community Land Model version 4.5 and the Community
112 Atmosphere Model version 5 (CAM5) of the Community Earth System Model (CESM)
113 version 1 (Zou et al., 2019; Neale et al., 2013) to perform two-way coupled simulations.
114 RESFire provides state-of-the-art capabilities to simulate the complex fire-climate-ecosystem
115 interactions globally for fires occurring over wildland, cropland, and peatland. Although
116 wildfires dominate in the North American region, RESFire simulates both wildfires and

117 prescribed fires. Moreover, this integrated setup includes climatic feedback from fire-induced
118 aerosol direct and indirect radiative effects and associated weather changes. It also includes
119 feedback from fire-induced vegetation distribution changes and associated biophysical
120 processes such as evapotranspiration and surface albedo. Sofiev et al. (2012) described the
121 fire plume rise parameterization. Other features in CLM4.5 and CAM5, such as the
122 photosynthesis scheme (Sun et al., 2012), the MAM3 aerosol module (Liu et al., 2012), and
123 the cloud macrophysics scheme (Park et al., 2014), allow for more comprehensive
124 assessments of the climate effects of fires through their interactions with vegetation and
125 clouds. Fire-ecosystem interactions are modelled by simulating fire-induced vegetation
126 mortality and regrowth (and associated land cover change) in RESFire. This approach has
127 been introduced in Zou et al. (2019) and the simulated ecological and climatic effects of
128 wildfires have been evaluated in two sets of sensitivity experiments in Zou et al. (2020).
129 Although fire-climate-ecosystem interactions are considered in this study, our focus is on the
130 fire-induced changes in PM_{2.5} over Canada and the US, so the two vegetation-focused
131 sensitivity experiments reported in Zou et al. (2020) are not included in this paper. Please
132 refer to Zou et al. (2019) and Zou et al. (2020) for more details about the simulation of fire-
133 ecosystem interactions.

134 **2.2 Numerical Experiment and Methodology**

135 We designed two sets of simulations for the present day and future scenarios to
136 quantify the impacts of fire-climate-ecosystem interactions (Table 1). The spatial resolution is
137 0.9° (lat) × 1.25° (lon) with a time step of 30 min. In each set of simulations, we conducted a
138 default all emission included control run (X_{ALL}, where x=2000 or 2050 indicates the present
139 day or future, respectively) and a sensitivity run with no wildfire emissions to the atmosphere
140 (X_{WEF}, where X is the same as for the control runs). The ALL runs are designed to simulate
141 fully interactive fire disturbances such as fire emissions with plume rise and fire induced land

142 cover changes of the present day (representative of the 2000s, 2000_{ALL}) and a moderate future
 143 emission scenario (representative of the 2050s, 2050_{ALL}) via the RCP4.5. The only difference
 144 between the ALL and WEF scenario is that wildfire emissions are absent in the WEF
 145 scenario. Specifically, in the WEF runs, the online simulated fire emissions are not passed to
 146 the CAM5 atmosphere model so that the difference between the ALL and WEF runs can be
 147 used to isolate the atmospheric impacts of fire-climate interactions.

148 Table 1: Summary of the sensitivity simulations performed

Scenario	Present-day		Future	
Experiment Name	2000 _{ALL}	2000 _{WEF}	2050 _{ALL}	2050 _{WEF}
Simulation years	2001-2010	2001-2010	2051-2060	2051-2060
Atmosphere	CAM5	CAM5	CAM5	CAM5
Land	CLM4.5	CLM4.5	CLM4.5	CLM4.5
Ocean	Climatology	Climatology	RCP4.5	RCP4.5
Sea ice	Climatology	Climatology	RCP4.5	RCP4.5
Non-fire emissions	ACCMIP	ACCMIP	RCP4.5	RCP4.5
Fire emissions	Online fire aerosols with plume rise	—	Online fire aerosols with plume rise	—
Land cover	Fire disturbances on present-day condition	Fire disturbances on present-day condition	Fire disturbances on RCP4.5 condition	Fire disturbances on RCP4.5 condition

149
 150 For the present-day experiments, we used the spun-up states from Zou et al. (2019) as
 151 initial conditions for both meteorological and chemical variables. Sea surface temperature
 152 (SST) for the present day was obtained from the Met Office Hadley Centre (HadISST).
 153 Present-day non-fire emissions from anthropogenic and other sources were based on
 154 ACCMIP (Lamarque et al., 2010) for the year 2000. We replaced the prescribed GFED2 fire
 155 emissions (van der Werf et al., 2006) in the default setting of CESM with the online-coupled
 156 fire emissions generated by the RESFire model. Zou et al. (2019) provided more details of
 157 the physics parameterizations and modeling experiment settings used in these simulations.

158 Land use and land cover data for 2000 and 2050 from the Land-Use History A product (Hurtt
159 et al., 2006) are used to initialize the 2000_{ALL}/2000_{WEF} and 2050_{ALL}/2050_{WEF} simulations,
160 respectively. Following the above setup, the future scenario 2050_{ALL} experiment accounts for
161 both fuel load changes associated with the projected land use and land cover change
162 (LULCC) in the 2050s and fire weather changes driven by the SST and sea ice forcing from a
163 coupled CESM simulation following the greenhouse gas (GHG) forcing of the RCP4.5
164 scenario. The global mean GHG mixing ratios in the CAM5 atmosphere model were fixed at
165 the year 2000 levels in all the present-day experiments and they were replaced by those of the
166 RCP4.5 scenario with the well-mixed assumption and monthly variations. However, the
167 future population and socioeconomic conditions were identical to those of the present day so
168 there was no explicit impact of human-induced mitigation/enhancement effects on wildfires
169 in the future projection in all the future experiments. Future human impacts were considered
170 implicitly in LULCC-induced fuel load changes in the RCP4.5 scenario.

171 The net projected changes by 2050s in emissions, meteorology and air quality during
172 summer (JJA: June, July, August) months are estimated by comparing decadal-mean values
173 simulated by 2000_{ALL} with 2050_{ALL}. Wildfire-induced enhancement in PM_{2.5} concentration in
174 the present day and mid-21st century is estimated by comparing 2000_{ALL} with 2000_{WEF} and
175 2050_{ALL} with 2050_{WEF}, respectively. Further, the projected increase in wildfire-induced
176 PM_{2.5} in the future is calculated by comparing the simulated wildfire effect of the 2050s
177 (2050_{ALL}-2050_{WEF}) with that of the 2000s (2000_{ALL}-2000_{WEF}). With large spatiotemporal
178 variability, the projected changes in transported fire-emissions from the western US and
179 Canada to the eastern US by the 2050s and the corresponding impacts are summarized using
180 probability distribution functions. The latter provide information not only for the mean but
181 also variability and extreme values to quantify the simulated changes for the three subregions.

182

183 **3. Results and Discussion**

184 **3.1 Model Evaluation**

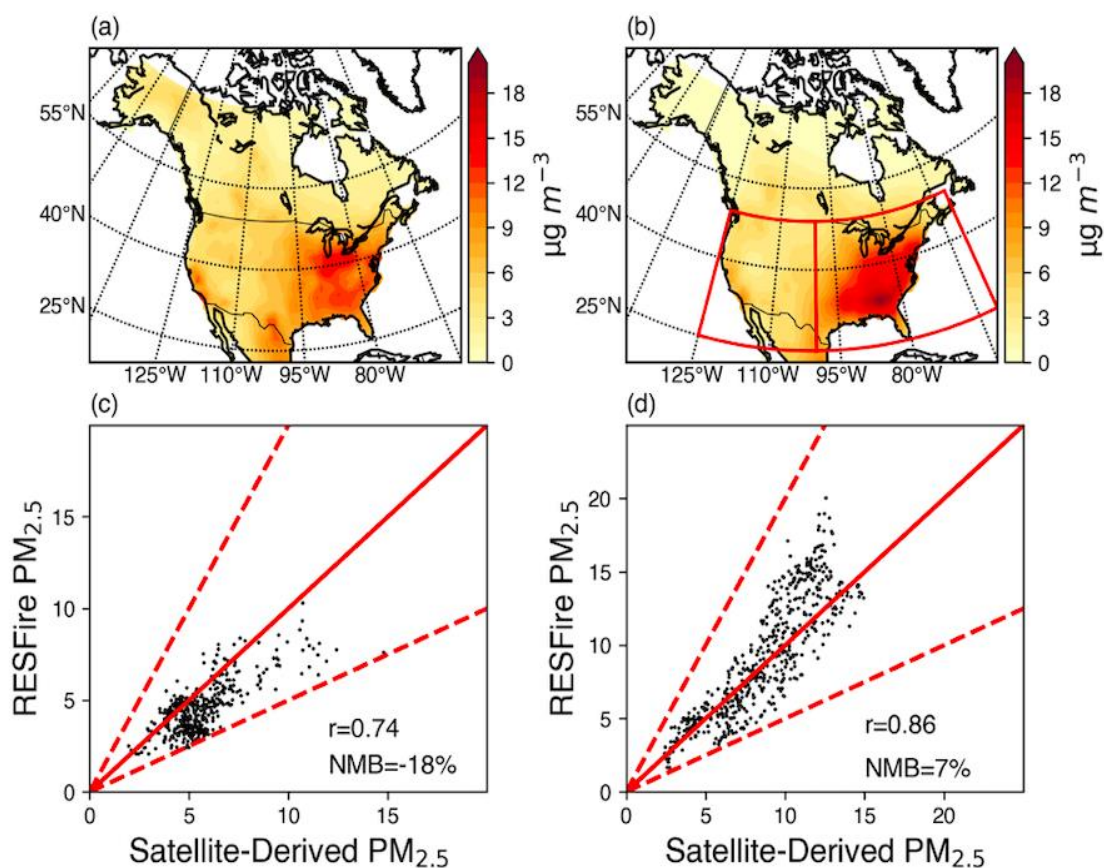
185 Zou et al. (2019) performed comprehensive evaluation of the RESFire simulated
186 wildfire burnt area distribution, associated carbon emissions and terrestrial carbon balance to
187 demonstrate reasonable model skill. Zou et al. (2020) compares global fire simulations by
188 CESM-RESFire with modeling results reported in the literature to show better agreement
189 with the GFED4.1s benchmark data and predicts more prominent changes in the future than
190 those predicted by Kloster et al. (2010, 2012). These differences might come from differences
191 in the climate sensitivities of the fire models and scenarios and other input data used to make
192 future projections.

193 Here, we evaluate the simulated surface PM_{2.5} against satellite-estimates (Figure 1)
194 over North America. The PM_{2.5} concentration is calculated as the sum of sulfate, nitrate, fine
195 sea salt (first 2 size bins), fine dust (first size bin), black carbon (BC), and organic aerosol
196 (OC) at the surface-level of model. OC is the sum of primary organic matter (POM) and
197 secondary organic aerosol (SOA), and SOA is the sum of secondary species formed from
198 toluene, monoterpenes, isoprene, benzene, and xylene. Figure 1 compares the observed and
199 simulated mean annual PM_{2.5} averaged over 2001-2010. The 10-year average satellite AOD-
200 derived annual mean surface PM_{2.5} concentrations (Van Donkelaar et al., 2018) are regridded
201 to the model grid (Figure 1A) and then compared with the RESFire simulations in the
202 2000_{ALL} present-day run (Figure 1B). The spatial distribution of annual surface PM_{2.5} is
203 reasonably well simulated but also have some biases. To quantify the biases, we also
204 estimated the correlation coefficient as well as normalized mean biases (NMB) of the
205 simulated values compared against the satellite retrieved values over two subregions.
206 Quantitatively, the NMB values over the western US (WUS) and eastern US (EUS) are 18%
207 and 7%, respectively (Figure 1C-D). In addition, the spatial variability of the 2001-2010

208 averaged annual AOD distribution (Supplementary Figure 1) is also well represented in our
209 simulation, although the model underestimates high AOD values. Similar spatial variability
210 and biases in AOD and PM_{2.5} were also found when a comparison was performed for only
211 summer months (June through August; JJA). The simulated PM_{2.5} has also been evaluated
212 against the ground-based Interagency Monitoring of Protected Visual Environments
213 (IMPROVE) data, showing similar spatial pattern and biases (10-25%) (Supplementary
214 Figure 2). The biases are smaller over Eastern US and Southwestern US region. The
215 simulated PM_{2.5} values over California matches quite well with the observed annual mean
216 values. However, the biases over Northwestern US region are ~30-40%, a portion of which
217 could be attributed to possible biases in model's meteorology in northwestern US region.
218 Nonetheless, both satellite and in situ evaluation indicate that our simulation biases are
219 largely within the uncertainty range among the various satellite and ground-based datasets,
220 which have normalized mean biases ranging from -3.3% to 33.3% when benchmarked against
221 the ground-based IMPROVE data over the contiguous US (Diao et al., 2019; Val Martin et al.
222 (2015)).

223 Discrepancies between the simulated and observed PM_{2.5} values may be attributed to
224 several potential reasons. First, the satellite-derived data has a non-zero lower bound of PM_{2.5}
225 concentrations, so the ambient background concentrations for relatively cleaner regions such
226 as the western US may be overestimated (Figure 1C), also the sampling frequency between
227 these datasets are different. Second, year 2000-based constant non-fire emissions were used
228 in the RESFire simulation, which may result in overestimation of the PM_{2.5} concentrations
229 from non-fire sources during 2001-2010 when anthropogenic emissions and PM_{2.5}
230 concentrations continue to decrease (US EPA, 2018). This overestimation is prominent in
231 regions dominated by non-fire sources such as the southeastern US. Third, large uncertainties
232 in fuel consumption and emission factors preclude an accurate estimation of the primary fire

233 emissions in the model, especially for the eastern US where large fractions of low-intensity
 234 prescribed fires consume only under-canopy fuels such as litter and duff layers. The fire
 235 model may fail to capture the subtle distinctions between low-intensity prescribed fires and
 236 forest fires, so more fuels are consumed and result in higher emissions. Lastly, comparison of
 237 a coarsely resolved simulation against in-situ observations also contributes to uncertainty.
 238 Differences in the degree to which fire-climate interactions and other physical processes and
 239 feedbacks are represented by the models can explain the slight differences in estimating the
 240 present day mean wildfire-induced change in PM_{2.5} over local and downwind regions
 241 between our simulations and previous studies. Nonetheless, reasonable simulation of the
 242 spatial distribution of wildfire burnt area, AOD, and near surface particulate concentration
 243 (mean bias of ~10-20 %) instills confidence about the fidelity of our model setup in
 244 particulate pollution simulation, which is the focus of this study.



245

246

247 Figure 1: Comparison of the 10-year (2001-2010) averaged annual mean surface PM_{2.5}
248 concentration between observations and RESFire simulations. (a) Satellite-derived surface
249 PM_{2.5} concentrations (with dust and sea-salt removed) estimated by Donkelaar et al., 2018
250 (available at [https://sedac.ciesin.columbia.edu/data/set/sdei-global-annual-gwr-pm2-5-modis-](https://sedac.ciesin.columbia.edu/data/set/sdei-global-annual-gwr-pm2-5-modis-misr-seawifs-aod)
251 [misr-seawifs-aod](https://sedac.ciesin.columbia.edu/data/set/sdei-global-annual-gwr-pm2-5-modis-misr-seawifs-aod); last access: 5 November, 2021); (b) 2000_{ALL} Simulated surface PM_{2.5}
252 concentrations (with dust and sea-salt removed) averaged over 2001-2010; The red boxes
253 denote the two subregions (EUS and WUS) shown in Fig. 2 in the main text. (c) comparison
254 of simulated and satellite based gridded surface PM_{2.5} concentrations in the WUS subregion;
255 Number of samples is equal to the number of land grids ~450 (d) same as (c) but in the EUS
256 subregion. Number of samples is equal to the number of land grids ~375 The red solid and
257 dashed lines denote the 1:1 ratio line and $\pm 100\%$ biases, respectively. The correlation
258 coefficients and NMB values are shown at the lower-right corner of each subplot.

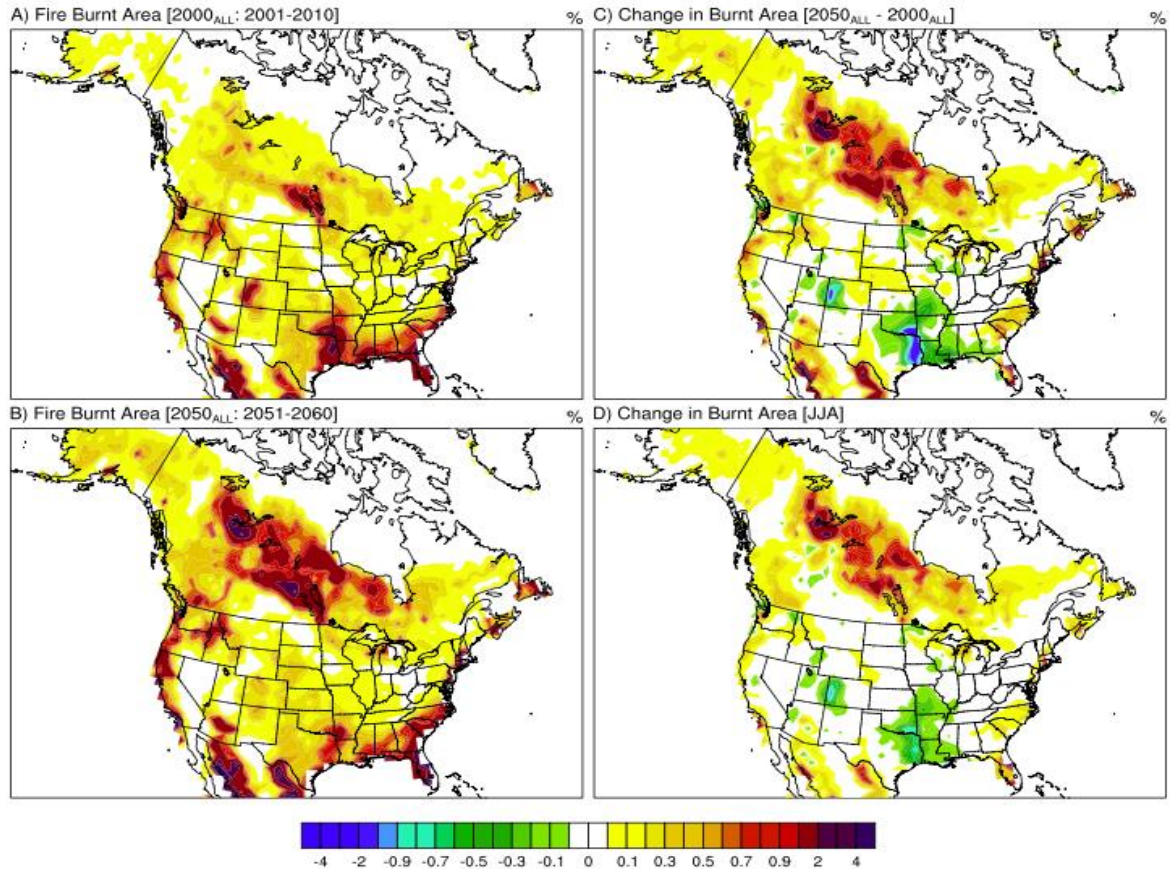
259

260 **3.2 Fire-induced changes in burnt area and PM_{2.5}**

261 The decadal-mean annual fire burnt area simulated for the present day shows
262 widespread wildfires over the entire North America (Figure 2A). Specifically, Canada and the
263 forested areas of the northwestern (> 36 N latitude) and southeastern (< 36 N latitude) US are
264 most intensely affected by wildfires in the present day. By the mid-21st century, a striking
265 increase of 2-5 times in fire burnt area is projected over Canada, Alaska, the Pacific
266 Northwest and portions of the western US by the 2050s (Figure 2B). A distinct positive shift
267 in the probability density function (PDF) of annual fire burnt area is evident in the future,
268 with the decadal-mean difference statistically significant at the 99% confidence level (Zou et
269 al., 2020). A small and statistically insignificant change in interannual variability (~ 0.4 Mha
270 yr⁻¹) of fire burnt areas is also simulated between the present and future. Specifically, our
271 model predicts more than a doubling of burnt area in boreal regions of Canada in the future,
272 in line with a previous projection for Canada (Wotton et al., 2017). Future enhancement in
273 fire burnt area is ~ 20-50% in most fire grids over the western coast of US, which is higher
274 than that over the eastern US (Figures 2A and 2C). The increase over the western US is closer
275 to the lower bound of that derived from statistical model ensemble projections for the western
276 US in the mid-21st century (Yue et al., 2013). The statistics-based projections of future burnt

277 area over North America were likely too high because fire-induced land cover change, fuel
278 load reduction and factors could induce a negative fire feedback, which was not considered in
279 previous fire projection studies (Zou et al. 2020).

280 Annual fire burnt area in the southeastern US shows a decline in the future (Figure
281 2C), as precipitation is projected to increase in that region (discussed later). Note that all
282 future fire changes between 2050_{ALL} and 2000_{ALL} are primarily associated with climate
283 warming in response to the increase in greenhouse gas (GHG) concentrations in the RCP4.5
284 scenario. No direct impacts of population and socioeconomic changes on wildfires are
285 included in our simulations, although these factors contribute to changes in GHG emissions
286 (via the RCP scenario) that influence the climate simulated in 2000_{ALL} and 2050_{ALL}. As about
287 80% of the projected fire changes in the future is restricted to the summer season (June
288 through August; JJA) (Figure 2D), we focus on analysis of the summer-mean wildfire-
289 induced PM_{2.5} and its projected future changes over North America.



290

291 **Figure 2: Spatial distribution of fire burnt area.** **A-D**, Spatial distribution of simulated
 292 decadal-mean annual burnt area (as percentage) over North America for present day (A),
 293 mid-21st century (B) and the net change between the 2050s and the 2000s (C). **D**, same as
 294 (C), but for wildfire burnt area during summer only (June through August; JJA). The colorbar
 295 illustrate grid fraction of area burnt.

296

297

The simulated 10-year averaged summer-mean wildfire-induced PM_{2.5} values in

298 2000_{ALL} are more than 0.5 μg/m³ over a large part of North America in the present day, with

299 noticeably larger values (> 1 μg/m³) in Canada and the northwestern, central, and

300 southeastern US (Figure 3A). Interestingly, the spatial distribution of wildfire-induced

301 PM_{2.5} > 1 μg/m³ resembles an inverted horse-shoe shape. The inverted horse-shoe shaped

302 spatial distribution is also consistent with the wildfire-smoke climatology derived from the

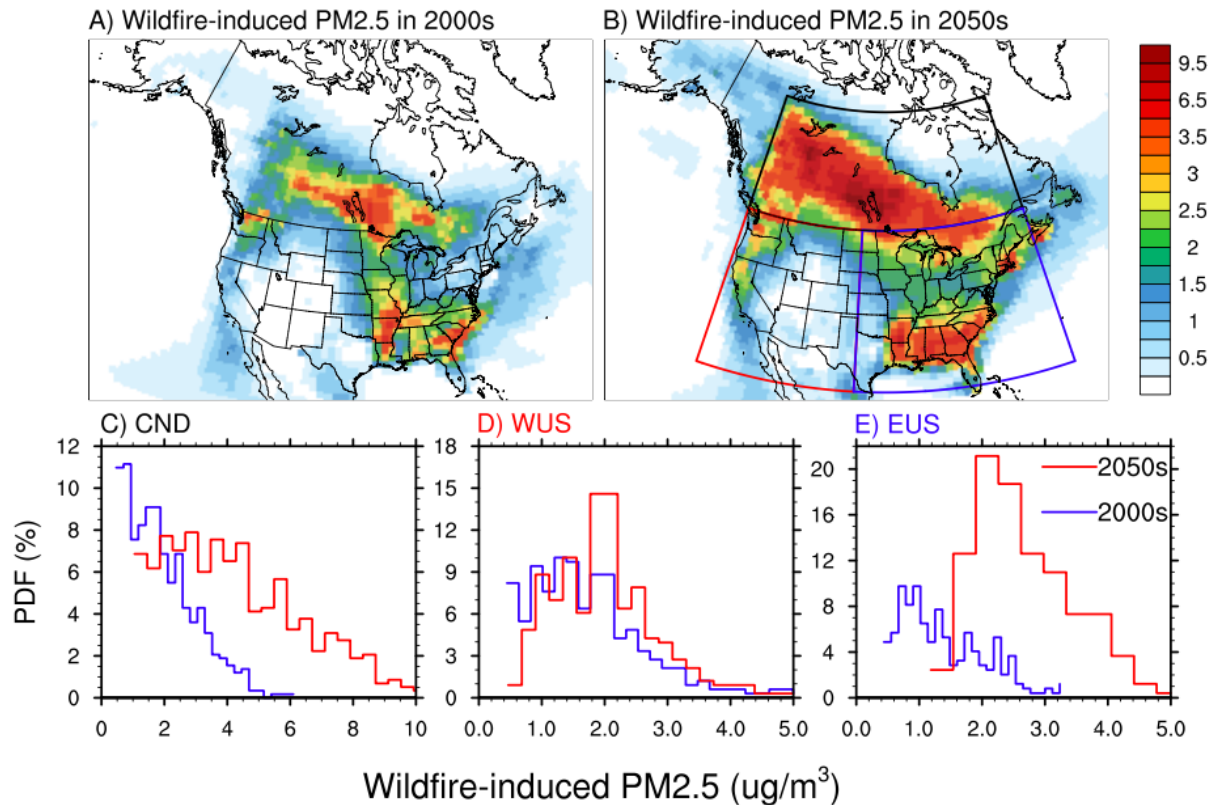
303 satellite-guided operational smoke product of the Hazard Mapping System (HMS) during

304 2005-2015 (Brey et al., 2018; Kaulfus et al., 2017). By the mid-21st century, the spatial extent

305 of the horse-shoe shape for areas with wildfire-induced PM_{2.5} enhancement > 1 μg/m³

306 expands significantly to span most regions of North America, with the most pronounced
307 enhancement occurring over Canada (Figure 3B). The PDFs of the spatial distribution for the
308 three regions can be seen in Figure 3C-E. Specifically, wildfire induced $PM_{2.5}$ in the 2000s
309 over Canada, WUS and EUS during summer is $\sim 1-3 \mu g/m^3$, $1-3 \mu g/m^3$ and $0.6-1.2 \mu g/m^3$,
310 respectively. Maximum values within the WUS region are found over the Pacific Northwest,
311 with most areas having wildfire induced $PM_{2.5}$ values of $\sim 2-3 \mu g/m^3$. Similarly, the southern
312 states have relatively high wildfire induced $PM_{2.5}$ concentrations of $\sim 2-4 \mu g/m^3$ within the
313 EUS in the present-day simulation.

314 Compared to the 2000s, the wildfire induced JJA-averaged $PM_{2.5}$ values are almost
315 doubled to $\sim 3-6 \mu g/m^3$ over Canada in the 2050s (Figure 3B and Figure 3C). Consistently,
316 the values of wildfire induced $PM_{2.5}$ over WUS (mainly coastal) also doubled in 2050s
317 compared to 2000s, with modal values of $\sim 2-2.5 \mu g/m^3$ (Figure 3D). Most interestingly, the
318 enhancement in wildfire-induced summer-mean $PM_{2.5}$ over the northern EUS is also
319 significant by the 2050s (Figures 3B). Largely, the summer-mean wildfire-induced $PM_{2.5}$
320 concentration over EUS increases from ~ 0.8 to $\sim 2 \mu g/m^3$ in the mid-century to values of $1.2-$
321 $3.0 \mu g/m^3$ (Figure 3E). The summer-mean wildfire-induced $PM_{2.5}$ is thus projected to double
322 in North America by the 2050s compared to the 2000s, with a substantial coverage over the
323 EUS. An important finding from these PDFs appears to be that there are fewer grids with < 1
324 $\mu g/m^3$ wildfire induced $PM_{2.5}$, or alternatively, that more regions are being influenced by
325 $PM_{2.5}$, and many areas that were already seeing wildfire impacts are seeing enhanced
326 impacts. Such enhancement is found not only at the surface but also in an elevated
327 atmospheric layer over EUS between 900 and 700 hPa. This is nonintuitive given the fact that
328 the increase in fire-burnt area by mid-century over the EUS is not substantial.



329

330 Figure 3: **Spatial distribution of PM_{2.5} concentrations.** Spatial distribution of decadal-mean
 331 wildfire-induced enhancement in summer (June through August; JJA) PM_{2.5} concentration
 332 over North America for present day (A, 2000_{ALL}-2000_{WEF}) and future (B, 2050_{ALL}-2050_{WEF}). **C-
 333 E**, Probability density functions (PDFs) of wildfire contribution within the three regions
 334 shown in Figure 2B for Canada (CND: black box) (C), WUS (red box) (D), and EUS (blue box)
 335 (E), respectively, for 2000s (blue) and 2050s (red). Only grids over land in North America are
 336 used to generate the PDFs. The y-axis indicates the probability of occurrence of different
 337 PM_{2.5} values shown in the x-axis. The colorbar illustrates PM_{2.5} in ug/m³.

338

339 As anthropogenic- and wildfire-induced PM_{2.5} concentrations may change differently

340 with time across North America, next, we investigate the relative contribution of wildfire-

341 induced PM_{2.5} to the total PM_{2.5} in the future. Prominent enhancement of the wildfire

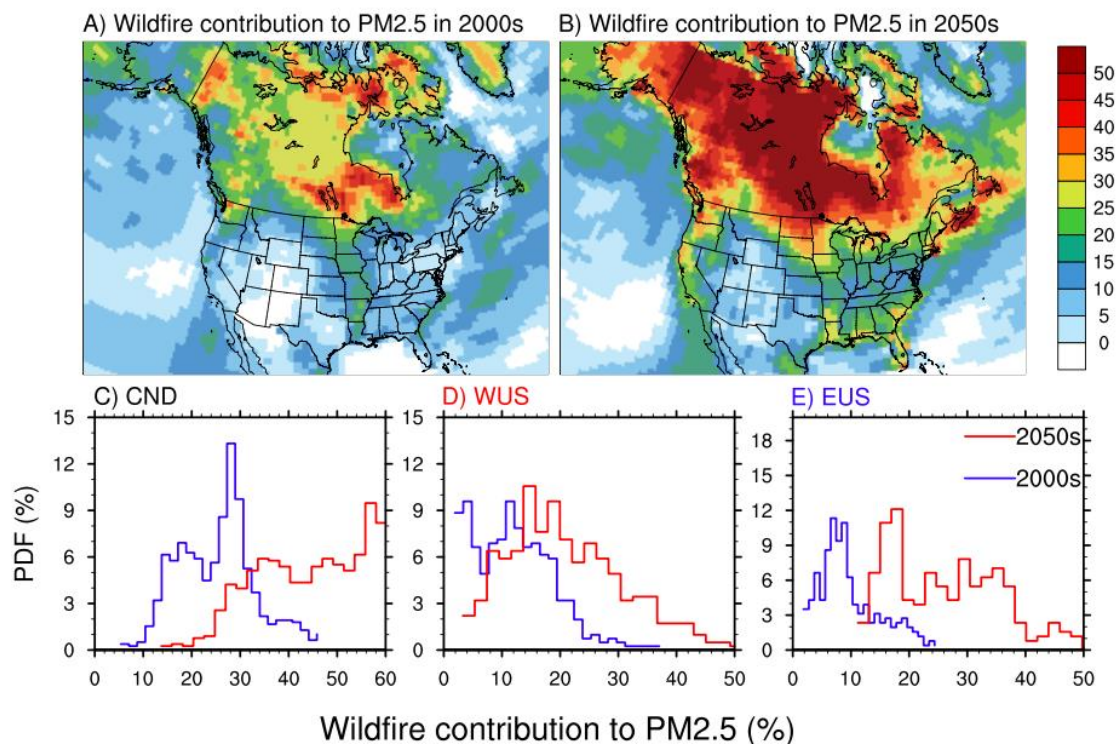
342 contribution is apparent in the entire domain by the 2050s (Figures 4A-B). Largely, during

343 the 2000s, the simulated fractional contribution of wildfires to PM_{2.5} is ~15-50 % in Canada

344 (Figure 4A). Specifically, a bi-modal distribution is simulated over Canada with modal values

345 around 18% and 30% (Figure 4C). Over WUS, the present day simulated percentage

346 contributions of wildfire-induced values are 5-25% (Figure 4A), with modal values between
 347 10-20% (Figure 4D). Note that many areas located in the Pacific Northwest have higher
 348 values of ~30-40% (Figure 4A). At the same time, the fractional contribution by wildfire-
 349 induced PM_{2.5} is ~5-10% in most areas of EUS in present day (Figure 4F). Nevertheless,
 350 some areas in the central US also have higher values of ~10-25% (Figure 4A).



351

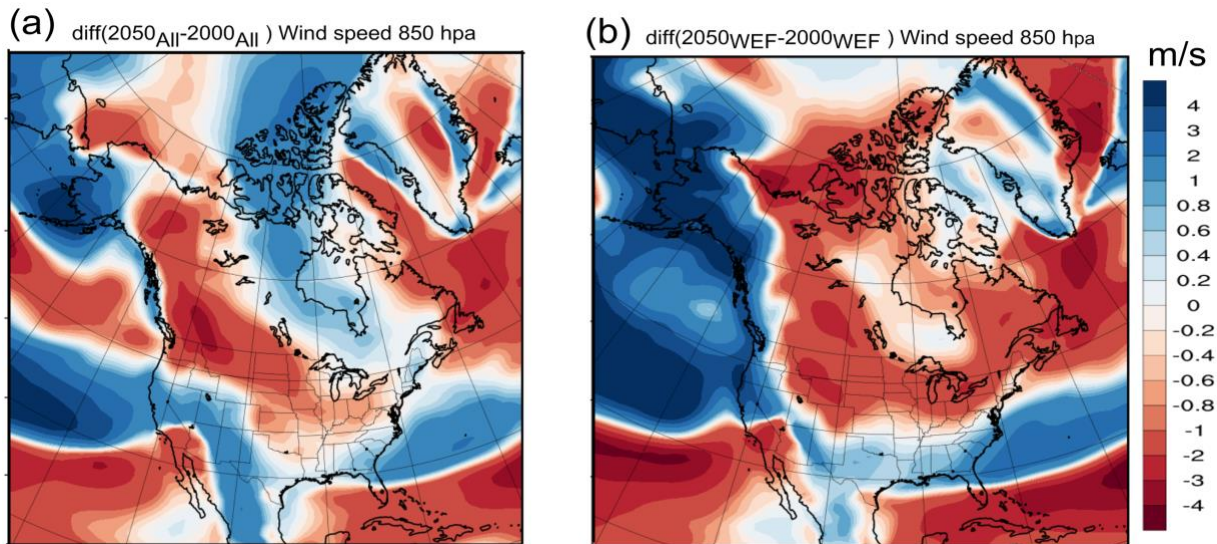
352 **Figure 4: Spatial distribution and probability density function of the percentage**
 353 **contribution of wildfire emissions. A-B**, Spatial distribution of the percentage contribution
 354 of wildfire emissions to decadal-averaged summer (June through August; JJA) mean PM_{2.5}
 355 concentrations over North America during present day (A) and future (B). The percentage
 356 contribution of wildfire-induced PM_{2.5} to the total PM_{2.5} concentrations is calculated as
 357 $([2000_{ALL}-2000_{WEF}]/2000_{ALL})$ and $([2050_{ALL}-2050_{WEF}]/2050_{ALL})$ for the present and future,
 358 respectively. **C-E**, Probability density functions (PDFs) of the percentage wildfire
 359 contribution within the three regions shown in Figure 2D for Canada (CND: black box) (C),
 360 WUS (red box) (D), and EUS (blue box) (E), respectively, for the 2000s (blue) and the 2050s
 361 (red). Only grids over land in North America are used to generate the PDFs. The y-axis
 362 indicates the probability of occurrence of different PM_{2.5} values shown in the x-axis.

363

364 The wildfire contributions in the 2050s show a clear shift towards higher values in all
365 sub-regions compared to the 2000s (Figure 4B). Over Canada, the values shifted from 15-30
366 % in the 2000s to ~30-60% in the 2050s, a nearly two-fold increase in the fractional
367 contribution of wildfire emissions to the total PM_{2.5} concentration is simulated (Figure 4B
368 and corresponding PDF in Figure 4C). Similarly, the contribution values increased to ~ 10-35
369 % in the 2050s, compared to 10-20% in the 2000s over WUS (Figure 4B), thereby featuring a
370 broadening of the bi-modal distribution of wildfire contribution (Figure 4D). The shift in the
371 percentage contribution is most prominent for the higher values, corresponding to some areas
372 located in the Pacific Northwest and west coast of the US (Figure 4B). Consistent with Figure
373 3B, the shift in the contribution values over EUS is also very distinct, revealing an increase in
374 the mode values from 6-10% in the 2000s to ~16-20 % by the 2050s (Figure 4B and Figure
375 4E). Thus, not only in absolute values, but our results also underscore a large increase in the
376 contribution of wildfire emissions over EUS in the future.

377 **3.3. Mechanistic understanding of the underlying processes**

378 The larger enhancement in the relative contribution of wildfire emissions to the total
379 surface PM_{2.5} in EUS in the 2050s can be explained by three mechanisms. First, due to the
380 increase in Canadian and western US wildfires, downwind transport of wildfire smoke
381 plumes to EUS will be enhanced by the 2050s. This long-range transport to the atmospheric
382 column of EUS can happen within a few days of the fire occurrence (Supplementary Figures
383 3A and 3B). Using Hazard Mapping System (HMS)-detected smoke plumes, recent studies
384 identified a strong positive association between the transported smoke plumes in the
385 atmospheric column and collocated surface PM_{2.5} enhancement in EUS (Brey et al., 2018;
386 Wu et al., 2018; Gunsch et al., 2018; Kaulfus et al., 2017; Larsen et al., 2017; Dempsey,
387 2013). Hazard Mapping System (HMS) is an operational smoke detection product over North



388

389 **Figure 5a: Spatial distribution of decadal mean summer (June through August; JJA) wildfire-induced**
 390 **future changes $[(2050_{\text{ALL}} - 2050_{\text{WEF}}) - (2000_{\text{ALL}} - 2000_{\text{WEF}})]$. A) Wind speed at 850 hpa for $[(2050_{\text{ALL}} -$**
 391 **$2000_{\text{ALL}}]$, B) Wind speed at 850 hpa $[(2050_{\text{WEF}}) - (2000_{\text{WEF}})]$.**

392 America known as developed by the National Oceanic and Atmospheric Administration
 393 (NOAA) and operated by National Environmental Satellite, Data, and Information Service
 394 (NESDIS), available at <http://satepsanone.nesdis.noaa.gov/FIRE/fire.html>. Specifically, these
 395 studies found that the smoke plumes transported from Canada are located at an altitude of ~
 396 1-3 km over EUS (Colarco et al., 2004; Wu et al., 2018). Due to mixing by the daytime
 397 boundary layer and deposition, the smoke plumes enhance the surface $\text{PM}_{2.5}$ concentration
 398 over EUS (Wu et al., 2018; Colarco et al., 2004; Rogers et al., 2020; Dreessen et al., 2015).
 399 Hence HMS smoky days may be a useful proxy for wildfire-induced surface $\text{PM}_{2.5}$ over
 400 North America. In agreement, Brey et al. (2018) showed that the HMS-based smoke plumes
 401 observed over EUS is significantly aged, suggestive of their long-range transport origin.
 402 Consistent with the observed temporal change in HMS pattern, Xue et al. (2021) estimated
 403 using the mid-visible Multi Angle Implementation of Atmospheric Correction (MAIAC)
 404 satellite-derived Aerosol Optical Depth (AOD) that Canadian and western US fires have
 405 caused an increase in the daily $\text{PM}_{2.5}$ over Montana, North Dakota, South Dakota and
 406 Minnesota by 18.3, 12.8, 10.4 and 10.1 $\mu\text{g m}^{-3}$, respectively, between August 2011 (a low

407 fire month) and August 2018 (a high fire month). In summary, the visually apparent satellite-
408 based signatures of wildfire-smoke across Canada and EUS provide a necessary, though not
409 sufficient, support for the influence of Canadian smoke plumes on EUS air quality. Although,
410 the change in burnt area over northeastern EUS is negligible compared to the western US and
411 Canadian regions, however, there are some enhancements seen over east coast of US, which
412 can also contribute to enhanced fire emissions.

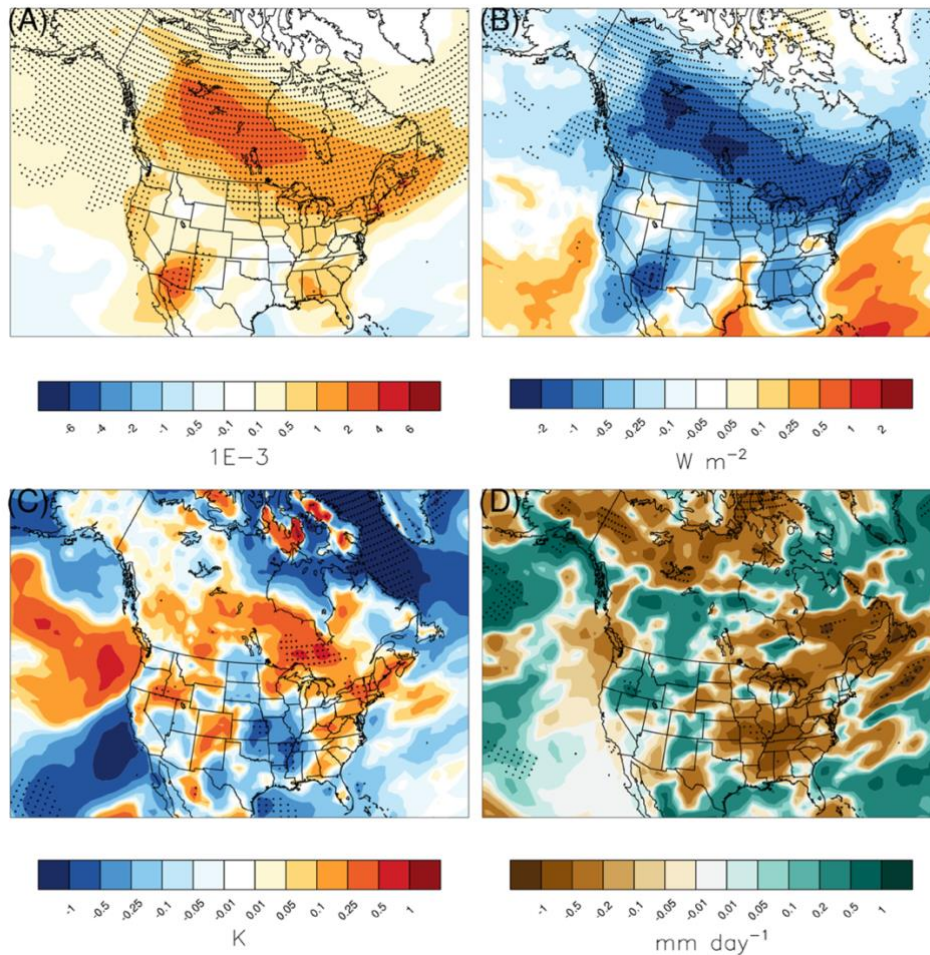
413 In future, the simulated speed of the westerly jet flows over Canada wildfire regions is
414 reduced in both the scenarios (Figure 5 A-B). It indicates that the westerly-induced
415 transported wildfire emissions from Canada boreal forests to the eastern half of Northern
416 America and EUS will be slower in future compared to that in present era. On the one hand, it
417 implies that the advection of smoke plumes will be slightly reduced in future. But on the
418 other hand, this phenomenon can also contribute to the enhanced PM_{2.5} values at surface as
419 these transporting plumes will be subject to relatively more boundary layer mixing over the
420 EUS and dry deposition/settling enhances. At the same time, the westerly winds over western
421 US below 40 °N is strengthened in future (Figure 5 A-B) compared to present day which
422 indicates more advection flux of wildfire emissions to EUS. Thus, the net effect is more
423 removal of wildfire-emitted PM_{2.5} from WUS and more influx of wildfire-emitted PM_{2.5} in
424 EUS.

425 Along with this dynamical changes, other climatic feedbacks simulated can also contribute to
426 enhancement of EUS pollution. Specifically, the enhancement of wildfire-induced smoke
427 aerosols increases solar absorption and scattering in the future (Figure 6A). This reduces the
428 incoming solar radiation reaching at the surface (Figure 6B) and induces surface cooling.
429 With atmospheric warming and surface cooling, lower-tropospheric stability is enhanced by
430 wildfire aerosols in the future (Figure 6C). The smoke plumes which reaches eastern US are

431 at an elevated altitude due to self-lofting property of absorbing aerosols as they travel
432 downwind but the smoke over western US is at near surface elevation as it is at its source
433 region. This can explain the more significant atmospheric stability simulated over the eastern
434 US compared to the source regions in western US and boreal forests of Canada. Relatively
435 stronger atmospheric stability over eastern US impose a stronger thermal capping that traps
436 more anthropogenic aerosols and particulate matter near the surface over EUS (already an
437 emission hotspot). At the same time, future increase in wildfire emissions also leads to
438 greater reduction of monthly rainfall (Figure 6D) over EUS, which may additionally
439 strengthen the positive feedback to surface PM_{2.5} over EUS by reducing wet scavenging of
440 transported wildfire smoke to EUS. Thus, wildfire-emitted aerosols induce positive feedback
441 on the surface PM_{2.5} concentration over EUS through fire-climate interactions that vary on a
442 regional scale. Moreover, the above discussed dynamical changes in future can also feedback
443 these simulated thermodynamical and precipitation changes, exaggerating the enhancement in
444 PM_{2.5} values over EUS in future. However, due to computational constrains, no direct
445 quantification of the magnitude of these feedback (with aerosol-radiation and aerosol-cloud
446 interactions turned off) on PM_{2.5} is performed and would be taken up in future studies.

447 Lastly, the reason of why the contribution of wildfire emissions to the total surface
448 PM_{2.5} in EUS is so substantial in the 2050s is the drastic reduction of anthropogenic
449 contribution to the surface PM_{2.5} over EUS in the future primarily due to policy-driven
450 reduction in anthropogenic emissions under the RCP4.5 scenario. Specifically, the simulated
451 ambient summer mean PM_{2.5} concentration exhibits widespread declines in the future
452 (Supplementary Figure 4), with reduction in PM_{2.5} concentration over eastern US in the range
453 of 4-15 $\mu\text{g}/\text{m}^3$, which is greatest within North America. Thus, large reduction in
454 anthropogenic contribution combined with increased downwind advection of Canadian

455 smoke to EUS and the associated positive feedbacks can explain the projected dominance of
456 wildfire emissions over EUS in future.



457
458 Figure 6: Spatial distribution of decadal mean summer (June through August; JJA) wildfire-
459 induced future changes [(2050_{ALL}-2050_{WEF}) - (2000_{ALL}-2000_{WEF})]. A) aerosol absorption
460 optical depth at 550 nm, B) aerosol direct radiative forcing at surface, C) lower-tropospheric
461 stability calculated as the difference between the potential temperature at 900 hPa and 1000
462 hPa, D) summer averaged precipitation rates, over North America. Areas marked with black dots
463 indicate grids where changes are significant at the 95% confidence level.

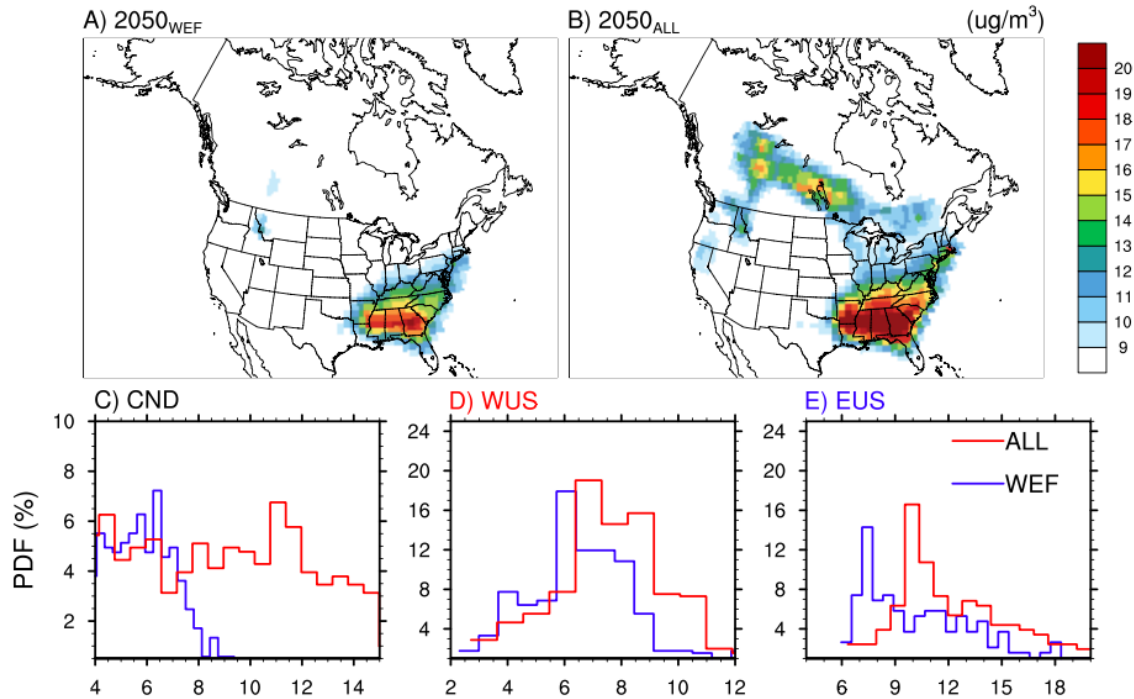
464

465 **3.4 Future Implications and uncertainties**

466 However, is the simulated future enhancement in wildfire contribution over EUS
467 substantial enough to affect the surface PM_{2.5} values over EUS in future? The World Health
468 Organization (WHO) air quality guidelines for annual and daily PM_{2.5} concentration are 10
469 μg m⁻³ and 25 μg m⁻³, respectively. As no specific guideline for seasonal-mean PM_{2.5} in the

470 summer is available, we use the annual guideline value as a reference to understand the
471 implication of wildfire emissions on ambient PM_{2.5} concentration in the future. Interestingly,
472 the mean summertime PM_{2.5} concentration in the wildfire emission free (WEF) scenario is
473 projected to remain within 10 µg m⁻³ over most of North America, except for the
474 southeastern US (~15% of the domain) (Figure 7A). However, the ALL-scenario projects an
475 increase in the exposure concentration level such that values > 10 µg/m³ are common in
476 Canada and EUS in the future (Figure 7B). Quantitatively, over Canada, the entire PDF of
477 PM_{2.5} concentration shifts towards higher values by ~5-6 µg/m³. Specifically, the modal value
478 shifts from ~ 6 µg/m³ in 2050_{WEF} to 11-12 µg/m³ in 2050_{ALL} (Figure 7C), so PM_{2.5}
479 concentration is projected to surpass the WHO guidelines over a large fraction of Canada in
480 the future. Similarly, the entire PDF of PM_{2.5} concentration shifts towards higher values by
481 ~2-3 µg/m³ over EUS, with the mode of the PDF increasing from ~ 7-8 µg/m³ in 2050_{WEF} to
482 ~ 10-11 µg/m³ in 2050_{ALL} (Figure 7E). The modal value of summer mean PM_{2.5} over WUS
483 increases from ~ 6 µg/m³ in 2050_{WEF} to ~ 7-8 µg/m³ in 2050_{ALL} (Figure 7D), although a few
484 grid cells show PM_{2.5} values greater than 10 µg/m³ (Figure 7B).

485 Clearly, the climate-induced enhancement in fires and its influence via the advected
486 wildfire smoke to EUS can have significant implications for air quality management in the
487 future. The PM_{2.5} enhancement in future over the southern states within EUS is large (Figure
488 7A-B), which is consistent with Figure 3 and 4 results. However, the future change in burnt
489 area over the same region is negligible or mostly reducing (Figure 1C-D). Thus, it can be
490 argued that the simulated enhancement is mostly related with the dynamic perturbations and
491 thermodynamical feedbacks due to wildfire emissions (Figure 6). As the rate of
492 anthropogenic emissions is also regionally highest over the Southeastern states, the impact of
493 these wildfire-induced climatic feedbacks on local air quality is distinctly seen over the EUS.



494

495 **Figure 7: Spatial distribution and probability density function of PM_{2.5} concentration in**
 496 **2050s. A-B**, Spatial distribution of decadal-average summer (June through August; JJA)
 497 mean PM_{2.5} concentration over North America in mid-21st century from 2050_{WEF} (wildfire
 498 emission-free) (A) and 2050_{ALL} (wildfire emission-inclusive) (B). **C-E**, Probability density
 499 functions (PDFs) of the same within the three regions shown in Figure 2B for Canada; CND
 500 (C), western US; WUS (D), and eastern US; EUS (E), respectively, for the 2050_{WEF} (blue)
 501 and 2050_{ALL} (red) runs. The y-axis indicates the probability of occurrence of different PM_{2.5}
 502 values shown in the x-axis. Only grids over land in North America are used to generate the
 503 PDFs. Note the different ranges of values shown in the y- and x-axis in **C-E**. The colorbar
 504 and the x-axis for Panel C-E indicates PM_{2.5} values.

505 Note that our simulated present-day estimates of wildfire induced PM_{2.5} values as well
 506 as the percentage contribution of wildfire emissions are within the range of reported values in
 507 previous studies over the domain, which augment the fidelity our future projections.

508 Specifically, our simulated present-day estimates of wildfire induced PM_{2.5} values are also
 509 within the range of reported values in previous studies over the domain. Reported values of
 510 wildfire-induced PM_{2.5} over WUS during summertime vary from $\sim 1 \mu\text{g}/\text{m}^3$ (Jaffe et al., 2008)
 511 to $\sim 2 \mu\text{g}/\text{m}^3$ (Park et al., 2007) and $\sim 3 \mu\text{g}/\text{m}^3$ (Ford et al., 2018), with the highest values
 512 documented over the Pacific Northwest and west coast regions ($\sim 1-4 \mu\text{g}/\text{m}^3$) (O'Dell et al.,
 513 2019). The wildfire-induced PM_{2.5} over EUS during summertime varies from $\sim 1 \mu\text{g}/\text{m}^3$ (Park

514 et al., 2007) to $\sim 2.5 \mu\text{g}/\text{m}^3$ ($\sim 3 \mu\text{g}/\text{m}^3$ in the southeastern US) (Ford et al., 2018).
515 Consistently, our simulated present-day estimates of wildfire contribution values are also
516 within the range of reported values in previous studies. For example, Meng et al. (2019)
517 found that wildfires can be the largest sectoral contributor ($\sim 18\text{-}59\%$) to the population-
518 weighted $\text{PM}_{2.5}$ in various subregions of Canada. Over WUS, the present-day percentage
519 contribution of wildfire induced $\text{PM}_{2.5}$ to the total $\text{PM}_{2.5}$ is reported to be $\sim 12\%$ (Liu et al.,
520 2017), $\sim 15\%$ (Park et al., 2007) and $\sim 30\%$ (Ford et al., 2018), with higher values of $\sim 40\%$ in
521 the Pacific Northwest (O'Dell et al., 2019). Over EUS our simulated values are also within
522 the range of previously reported values of $\sim 5\%$ (Park et al., 2007) and $\sim 15\text{-}18\%$ (Ford et al.,
523 2018). However, our two-way coupled simulations illustrate that future enhancement in the
524 wildfire associated $\text{PM}_{2.5}$ over the EUS could be greater compared to the western US, which
525 is not emphasized explicitly in any of the previous studies (although Ford et al., 2018
526 illustrated increase in $\text{PM}_{2.5}$ over mid and central US from Canadian fires). These could be
527 since inclusion of the wildfire-induced climatic feedbacks in our simulation is an
528 unprecedented exercise. Please also note that our study is focused on JJA period and the
529 wildfires in western US mainly occurs during August-September months, so the results
530 should be compared consciously.

531 Nonetheless, inherent limitations in our simulations may introduce uncertainties in the
532 projected future changes. For example, our reported changes in $\text{PM}_{2.5}$ concentrations based on
533 relatively coarse resolution simulations and decadal averages likely represent a low-end
534 estimate compared to changes at regional and daily/weekly scales. Moreover, our
535 experiments do not consider the direct human influences such as population change and
536 socioeconomic development on wildfires, which may aggravate the increase in $\text{PM}_{2.5}$
537 concentrations over the densely populated EUS in the future. Common sources of uncertainty
538 in modeling burnt area and fire emission and fire aerosol and smoke are also present in our

539 model. Fire smoke, in particular, is extremely hard to measure and evaluate. Lastly, inherent
540 uncertainties in the physics parameterizations used in the model, sensitivity of climate to
541 GHGs emissions, and the RCP scenarios should also be noted. Thus, ensemble modeling
542 considering different emissions scenarios, population and future time periods, and the use of
543 a finer spatial resolution may provide a more robust and better quantification of the wildfire-
544 induced impact on policy regulated improvements in PM_{2.5} over EUS.

545 **4. Conclusion**

546 In summary, online coupled fire-climate-ecosystem simulations project a nearly
547 twofold increase in wildfire-induced summer-mean surface PM_{2.5} concentration by the mid-
548 21st century over the entire North America. In a wildfire-emission free future, a large portion
549 of North America will have PM_{2.5} values below the WHO guidelines. But in a future with
550 wildfire emissions, the improvements from policy-driven reductions in anthropogenic PM_{2.5}
551 will be compromised by the projected doubling of PM_{2.5} from wildfires. More strikingly,
552 wildfire-induced enhancement in surface PM_{2.5} values and percentage contribution of the
553 wildfire emissions over EUS could be substantial by mid-century. This is mainly because of
554 the large enhancement in fires over Northern America by 2050s and associated increase in
555 amount of downwind transport of smoke to EUS. In addition, enhancement of smoke
556 transport induces a positive climate feedback to PM_{2.5} concentrations over EUS by increasing
557 the lower-tropospheric stability and reducing wet scavenging rates. Despite the inherent
558 limitations, this study highlights the natural versus anthropogenic contributions and the non-
559 local nature of air pollution that can complicate regulatory strategies aimed at improving air
560 quality over the eastern US in a warmer future.

561 **Data availability statements**

562 The HMS data used in this paper are available free through the link
563 <https://www.ospo.noaa.gov/Products/land/hms.html>. The model simulations data are
564 available at <https://portal.nersc.gov/project/m1660/yang560/wildfire>

565 **Code availability statements**

566 The model code and scripts are available at
567 <https://portal.nersc.gov/project/m1660/yang560/wildfire>

568

569 **Acknowledgements:**

570 This research was performed at PNNL and funded under Assistance Agreement No.
571 RD835871 by the U.S. Environmental Protection Agency to Yale University through the
572 SEARCH (Solutions for Energy, AiR, Climate, and Health) Center. It has not been formally
573 reviewed by EPA. The views expressed in this document are solely those of the SEARCH
574 Center and do not necessarily reflect those of the Agency. EPA does not endorse any
575 products or commercial services mentioned in this publication. CS is supported by the New
576 Faculty Initiation Grant project number CE/20-21/065/NFIG/008961 from IIT Madras.
577 PNNL is operated by Battelle Memorial Institute for the U.S. Department of Energy under
578 contract DE-AC06-76RLO-1830.

579

580 **Authors Contribution**

581 YQ, CS and RL designed this study. CS did the model and satellite analysis and wrote the
582 first draft of the manuscript. YZou performed the simulations. All authors provided inputs
583 throughout the study and helped in the drafting and submission process.

584

585 **References**

586 Abatzoglou, J. T. and Williams, A. P.: Impact of anthropogenic climate change on wildfire
587 across western US forests, *Proc. Natl. Acad. Sci.*, 113(42), 11770 LP – 11775,
588 doi:10.1073/pnas.1607171113, 2016.

589 Andela, N., Morton, D. C., Giglio, L., Chen, Y., van der Werf, G. R., Kasibhatla, P. S.,
590 DeFries, R. S., Collatz, G. J., Hantson, S., Kloster, S., Bachelet, D., Forrest, M., Lasslop, G.,
591 Li, F., Mangeon, S., Melton, J. R., Yue, C. and Randerson, J. T.: A human-driven decline in
592 global burned area, *Science* (80-.), 356(6345), 1356 LP – 1362,
593 doi:10.1126/science.aal4108, 2017.

594 Anjali, H., Muhammad, A., Anthony, D. M., Karen, S., R., S. M., Mick, M., M., T. A., J., A.
595 M. and Martine, D.: Impact of Fine Particulate Matter (PM_{2.5}) Exposure During Wildfires on
596 Cardiovascular Health Outcomes, *J. Am. Heart Assoc.*, 4(7), e001653,
597 doi:10.1161/JAHA.114.001653, 2019.

598 Black, C., Tesfaigzi, Y., Bassein, J. A. and Miller, L. A.: Wildfire smoke exposure and
599 human health: Significant gaps in research for a growing public health issue, *Environ.*
600 *Toxicol. Pharmacol.*, 55, 186–195, doi:<https://doi.org/10.1016/j.etap.2017.08.022>, 2017.

601 Brey, S. J., Ruminski, M., Atwood, S. A. and Fischer, E. V: Connecting smoke plumes to

602 sources using Hazard Mapping System (HMS) smoke and fire location data over North
603 America, *Atmos. Chem. Phys.*, 18(3), 1745–1761, doi:10.5194/acp-18-1745-2018, 2018.

604 Dempsey, F.: Forest Fire Effects on Air Quality in Ontario: Evaluation of Several Recent
605 Examples, *Bull. Am. Meteorol. Soc.*, 94(7), 1059–1064, doi:10.1175/BAMS-D-11-00202.1,
606 2013.

607 Dominici, F., Peng, R. D., Bell, M. L., Pham, L., McDermott, A., Zeger, S. L. and Samet, J.
608 M.: Fine Particulate Air Pollution and Hospital Admission for Cardiovascular and
609 Respiratory Diseases, *JAMA*, 295(10), 1127–1134, doi:10.1001/jama.295.10.1127, 2006.

610 Diao, M., Holloway, T., Choi, S., O’Neill, S.M., Al-Hamdan, M.Z., Van Donkelaar, A.,
611 Martin, R.V., Jin, X., Fiore, A.M., Henze, D.K. and Lacey, F., 2019. Methods, availability,
612 and applications of PM_{2.5} exposure estimates derived from ground measurements, satellite,
613 and atmospheric models. *Journal of the Air & Waste Management Association*, 69(12),
614 pp.1391-1414.

615 Ford, B., Val Martin, M., Zelasky, S. E., Fischer, E. V., Anenberg, S. C., Heald, C. L. and
616 Pierce, J. R.: Future Fire Impacts on Smoke Concentrations, Visibility, and Health in the
617 Contiguous United States, *GeoHealth*, 2(8), 229–247, doi:10.1029/2018GH000144, 2018.

618 Gillett, N. P., Weaver, A. J., Zwiers, F. W. and Flannigan, M. D.: Detecting the effect of
619 climate change on Canadian forest fires, *Geophys. Res. Lett.*, 31(18),
620 doi:10.1029/2004GL020876, 2004.

621 Gunsch, M. J., May, N. W., Wen, M., Bottenus, C. L. H., Gardner, D. J., VanReken, T. M.,
622 Bertman, S. B., Hopke, P. K., Ault, A. P. and Pratt, K. A.: Ubiquitous influence of wildfire
623 emissions and secondary organic aerosol on summertime atmospheric aerosol in the forested
624 Great Lakes region, *Atmos. Chem. Phys.*, 18(5), 3701–3715, doi:10.5194/acp-18-3701-2018,
625 2018.

626 Guan S, Wong DC, Gao Y, Zhang T, Pouliot G. Impact of wildfire on particulate matter in
627 the southeastern United States in November 2016. *Sci Total Environ.* 2020;724:138354.
628 doi:10.1016/j.scitotenv.2020.138354.

629 Johnston F. H., Henderson. S. B., Yang, C., T., R. J., Miriam, M., S., D. R., Patrick, K.,
630 M.J.S., B. D. and Michael, B.: Estimated Global Mortality Attributable to Smoke from
631 Landscape Fires, *Environ. Health Perspect.*, 120(5), 695–701, doi:10.1289/ehp.1104422,
632 2012.

633 Harris, R. M. B., Remenyi, T. A., Williamson, G. J., Bindoff, N. L., and Bowman, D. M. J.
634 S.: Climate-vegetation fire interactions and feedbacks: trivial detail or major barrier to
635 projecting the future of the Earth system?, *Wires Clim. Change*, 7, 910-931,
636 10.1002/wcc.428, 2016.

637 Hantson, S., Arneth, A., Harrison, S. P., Kelley, D. I., Prentice, I. C., Rabin, S. S., et al.
638 (2016). The status and challenge of global fire modelling. *Biogeosciences*, 13, 3359–3375.
639 <https://doi.org/10.5194/bg-13-3359-2016>

640 Hu, X., Yu, C., Tian, D., Ruminski, M., Robertson, K., Waller, L. A. and Liu, Y.:
641 Comparison of the Hazard Mapping System (HMS) fire product to ground-based fire records
642 in Georgia, USA, *J. Geophys. Res. Atmos.*, 121(6), 2901–2910, doi:10.1002/2015JD024448,
643 2016.

644 HURTT, G. C., FROLKING, S., FEARON, M. G., MOORE, B., SHEVLIAKOVA, E.,
645 MALYSHEV, S., PACALA, S. W. and HOUGHTON, R. A.: The underpinnings of land-use
646 history: three centuries of global gridded land-use transitions, wood-harvest activity, and
647 resulting secondary lands, *Glob. Chang. Biol.*, 12(7), 1208–1229, doi:10.1111/j.1365-
648 2486.2006.01150.x, 2006.

649 Jaffe, D., Hafner, W., Chand, D., Westerling, A. and Spracklen, D.: Interannual Variations in
650 PM_{2.5} due to Wildfires in the Western United States, *Environ. Sci. Technol.*, 42(8), 2812–
651 2818, doi:10.1021/es702755v, 2008.

652 Jolly, W. M., Cochrane, M. A., Freeborn, P. H., Holden, Z. A., Brown, T. J., Williamson, G.
653 J. and Bowman, D. M. J. S.: Climate-induced variations in global wildfire danger from 1979
654 to 2013, *Nat. Commun.*, 6, 7537 [online] Available from:
655 <https://doi.org/10.1038/ncomms8537>, 2015.

656 Kaulfus, A. S., Nair, U., Jaffe, D., Christopher, S. A. and Goodrick, S.: Biomass Burning
657 Smoke Climatology of the United States: Implications for Particulate Matter Air Quality,
658 *Environ. Sci. Technol.*, 51(20), 11731–11741, doi:10.1021/acs.est.7b03292, 2017.

659 Kirchmeier-Young, M. C., Zwiers, F. W., Gillett, N. P. and Cannon, A. J.: Attributing
660 extreme fire risk in Western Canada to human emissions, *Clim. Change*, 144(2), 365–379,
661 doi:10.1007/s10584-017-2030-0, 2017.

662 Kitzberger, T., Falk, D. A., Westerling, A. L. and Swetnam, T. W.: Direct and indirect
663 climate controls predict heterogeneous early-mid 21st century wildfire burned area across
664 western and North America, *PLoS One*, 12(12), e0188486 [online] Available from:
665 <https://doi.org/10.1371/journal.pone.0188486>, 2017.

666 Knorr, W., Dentener, F., Lamarque, J.-F., Jiang, L. and Arneth, A.: Wildfire air pollution
667 hazard during the 21st century, *Atmos. Chem. Phys.*, 17(14), 9223–9236, doi:10.5194/acp-
668 17-9223-2017, 2017.

669 Koplitz, S.N., Nolte, C.G., Pouliot, G.A., Vukovich, J.M. and Beidler, J., 2018. Influence of
670 uncertainties in burned area estimates on modeled wildland fire PM_{2.5} and ozone pollution
671 in the contiguous US. *Atmospheric environment*, 191, pp.328-339.

672 Lamarque, J. F., Bond, T. C., Eyring, V., Granier, C., Heil, A., Klimont, Z., Lee, D., Liousse,
673 C., Mieville, A., Owen, 628 B., Schultz, M. G., Shindell, D., Smith, S. J., Stehfest, E., Van
674 Aardenne, J., Cooper, O. R., Kainuma, M., 629 Mahowald, N., McConnell, J. R., Naik, V.,
675 Riahi, K., and van Vuuren, D. P.: Historical (1850–2000) gridded anthropogenic and biomass
676 burning emissions of reactive gases and aerosols: methodology and application, 631 *Atmos.*
677 *Chem. Phys.*, 10, 7017–7039, 10.5194/acp-10-7017-2010, 2010.

678 Leibensperger, E. M., Mickley, L. J., Jacob, D. J., Chen, W.-T., Seinfeld, J. H., Nenes, A.,
679 Adams, P. J., Streets, D. G., Kumar, N. and Rind, D.: Climatic effects of 1950–2050
680 changes in US anthropogenic aerosols – Part 2: Climate response, *Atmos. Chem.*
681 *Phys.*, 12(7), 3349–3362, doi:10.5194/acp-12-3349-2012, 2012.

682 Li, F., Zeng, X. D., & Levis, S. (2012). A process-based fire parameterization of intermediate
683 complexity in a dynamic global vegetation model. *Biogeosciences*, 9(7), 2761–2780.
684 <https://doi.org/10.5194/bg-9-2761-2012>

685 Liu, J. C., Mickley, L. J., Sulprizio, M. P., Dominici, F., Yue, X., Ebisu, K., Anderson, G. B.,
686 Khan, R. F. A., Bravo, M. A. and Bell, M. L.: Particulate Air Pollution from Wildfires in the

687 Western US under Climate Change, *Clim. Change*, 138(3), 655–666, doi:10.1007/s10584-
688 016-1762-6, 2016.

689 Liu, Y., Goodrick, S. and Heilman, W.: Wildland fire emissions, carbon, and climate:
690 Wildfire–climate interactions, *For. Ecol. Manage.*, 317, 80–96,
691 doi:<https://doi.org/10.1016/j.foreco.2013.02.020>, 2014.

692 Liu, X., Easter, R. C., Ghan, S. J., Zaveri, R., Rasch, P., Shi, X., Lamarque, J. F., Gettelman,
693 A., Morrison, H., Vitt, F., Conley, A., Park, S., Neale, R., Hannay, C., Ekman, A. M. L.,
694 Hess, P., Mahowald, N., Collins, W., Iacono, M. J., Bretherton, C. S., Flanner, M. G., and
695 Mitchell, D.: Toward a minimal representation of aerosols in climate models: description and
696 evaluation in the Community Atmosphere Model CAM5, *Geosci. Model Dev.*, 5, 709- 652
697 739, 10.5194/gmd-5-709-2012, 2012.

698 Meng, J., Martin, R.V., Li, C., van Donkelaar, A., Tzompa-Sosa, Z.A., Yue, X., Xu, J.W.,
699 Weagle, C.L. and Burnett, R.T., 2019. Source Contributions to Ambient Fine Particulate
700 Matter for Canada. *Environmental science & technology*, 53(17), pp.10269-10278.

701 McClure, C. D. and Jaffe, D. A.: US particulate matter air quality improves except in
702 wildfire-prone areas, *Proc. Natl. Acad. Sci.*, 115(31), 7901 LP – 7906,
703 doi:10.1073/pnas.1804353115, 2018.

704 Neale, R. B., Chen, C. C., Gettelman, A., Lauritzen, P. H., Park, S., Williamson, D. L.,
705 Conley, A. J., Garcia, R., Kinnison, D., Lamarque, J. F., Marsh, D., Mills, M., Smith, A. K.,
706 Tilmes, S., Vitt, F., Morrison, H., Cameron671 Smith, P., Collins, W. D., Iacono, M. J.,
707 Easter, R. C., Ghan, S. J., Liu, X. H., Rasch, P. J., and Taylor, M. A.: Description of the
708 NCAR Community Atmosphere Model (CAM 5.0), NCAR 289, 2013

709 Nolte, C. G., Spero, T. L., Bowden, J. H., Mallard, M. S. and Dolwick, P. D.: The potential
710 effects of climate change on air quality across the conterminous US at 2030 under three
711 Representative Concentration Pathways, *Atmos. Chem. Phys.*, 18(20), 15471–15489,
712 doi:10.5194/acp-18-15471-2018, 2018.

713 Katelyn O’Dell, Bonne Ford, Emily V. Fischer, and Jeffrey R. Pierce *Environmental Science*
714 & *Technology* 2019 53 (4), 1797-1804, DOI: 10.1021/acs.est.8b05430.
715

716 Partain, J. L., Alden, S., Strader, H., Bhatt, U. S., Bieniek, P. A., Brettschneider, B. R.,
717 Walsh, J. E., Lader, R. T., Olsson, P. Q., Rupp, T. S., Thoman, R. L., York, A. D. and Ziel,
718 R. H.: An Assessment of the Role of Anthropogenic Climate Change in the Alaska Fire
719 Season of 2015, *Bull. Am. Meteorol. Soc.*, 97(12), S14–S18, doi:10.1175/BAMS-D-16-
720 0149.1, 2016.

721 Park, S., Bretherton, C. S., and Rasch, P. J.: Integrating Cloud Processes in the Community
722 Atmosphere Model, Version 5, *J. Climate*, 27, 6821-6856, 10.1175/Jcli-D-14-00087.1, 2014.

723 Park, R.J., Jacob, D.J. and Logan, J.A., 2007. Fire and biofuel contributions to annual mean
724 aerosol mass concentrations in the United States. *Atmospheric Environment*, 41(35), pp.7389-
725 7400.

726 Pierce, J. R., Val Martin, M., & Heald, C. L. (2017). Estimating the Effects of Changing
727 Climate on Fires and Consequences for U.S. Air Quality, Using a Set of Global and Regional
728 Climate Models (final report no. JFSP-13-1-01-4). Retrieved from
729 https://www.firescience.gov/projects/13-1-01-4/project/13-1-01-4_final_report.pdf

730 Pouliot G, Pace TG, Roy B, Pierce T, Mobley D. Development of a biomass burning
731 emissions inventory by combining satellite and ground-based information. *J Appl Remote*
732 *Sens.* 2008;2:021501. doi: 10.1117/1.2939551.

733 Randerson, J. T., Chen, Y., van der Werf, G. R., Rogers, B. M., & Morton, D. C. (2012).
734 Global burned area and biomass burning emissions from small fires. *Journal of Geophysical*
735 *Research*, 117, G04012. <https://doi.org/10.1029/2012JG002128>

736 Rolph, G. D., Draxler, R. R., Stein, A. F., Taylor, A., Ruminski, M. G., Kondragunta, S.,
737 Zeng, J., Huang, H.-C., Manikin, G., McQueen, J. T. and Davidson, P. M.: Description and
738 Verification of the NOAA Smoke Forecasting System: The 2007 Fire Season, *Weather*
739 *Forecast.*, 24(2), 361–378, doi:10.1175/2008WAF2222165.1, 2009.

740 Spracklen, D. V., Mickley, L. J., Logan, J. A., Hudman, R. C., Yevich, R., Flannigan, M. D.,
741 & Westerling, A. L. (2009). Impacts of climate change from 2000 to 2050 on wildfire activity
742 and carbonaceous aerosol concentrations in the western United States. *Journal of Geophysical*
743 *Research*, 114, D20301. <https://doi.org/10.1029/2008JD010966>

744 Sun, Y., Gu, L. H., and Dickinson, R. E.: A numerical issue in calculating the coupled carbon
745 and water fluxes in a climate model, *J. Geophys. Res.-Atmos.*, 117,
746 D2210310.1029/2012jd018059, 2012

747 Sofiev, M., Ermakova, T., and Vankevich, R.: Evaluation of the smoke-injection height from
748 wild-land fires using remote-sensing data, *Atmos. Chem. Phys.*, 12, 1995-2006, 10.5194/acp-
749 12-1995-2012, 2012

750 Shi, H., Jiang, Z., Zhao, B., Li, Z., Chen, Y., Gu, Y., Jiang, J. H., Lee, M., Liou, K.-N., Neu,
751 J. L., Payne, V. H., Su, H., Wang, Y., Witek, M. and Worden, J.: Modeling Study of the Air
752 Quality Impact of Record-Breaking Southern California Wildfires in December 2017, *J.*
753 *Geophys. Res. Atmos.*, 0(0), doi:10.1029/2019JD030472, 2019.

754 U.S. EPA (U.S. Environmental Protection Agency). 2009. Integrated Science Assessment
755 (ISA) For Particulate Matter (Final Report). EPA/600/R-08/139F. Washington, DC:U.S. EPA.

756 U.S. EPA. 2018. Our Nation's Air. <https://gispub.epa.gov/air/trendsreport/2018/>

757 Val Martin, M., Heald, C. L., Lamarque, J.-F., Tilmes, S., Emmons, L. K. and Schichtel, B.
758 A.: How emissions, climate, and land use change will impact mid-century air quality over the
759 United States: a focus on effects at national parks, *Atmos. Chem. Phys.*, 15(5), 2805–2823,
760 doi:10.5194/acp-15-2805-2015, 2015.

761 Van der Werf, G. R., Randerson, J. T., Giglio, L., Collatz, G. J., Kasibhatla, P. S., and
762 Arellano, A. F.: Interannual variability in global biomass burning emissions from 1997 to
763 2004, *Atmos. Chem. Phys.*, 6, 3423-3441, DOI 737 10.5194/acp-6-3423-2006, 2006

764 Van Der Werf, G. R., Randerson, J. T., Giglio, L., Collatz, G. J., Mu, M., Kasibhatla, P. S.,
765 Morton, D. C., Defries, R. S., Jin, Y. and Van Leeuwen, T. T.: Global fire emissions and the
766 contribution of deforestation, savanna, forest, agricultural, and peat fires (1997-2009), *Atmos.*
767 *Chem. Phys.*, 10(23), 11707–11735, doi:10.5194/acp-10-11707-2010, 2010.

768 Van Donkelaar, A., R. V. Martin, M. Brauer, N. C. Hsu, R. A. Kahn, R. C. Levy, A.
769 Lyapustin, A. M. Sayer, and D. M. Winker. 2018. Global Annual PM_{2.5} Grids from MODIS,
770 MISR and SeaWiFS Aerosol Optical Depth (AOD) with GWR, 1998-2016. Palisades NY:

771 NASA Socioeconomic Data and Applications Center (SEDAC).
772 <https://doi.org/10.7927/H4ZK5DQS>. Accessed 16 November 2019.

773 Ward, D. S., Kloster, S., Mahowald, N. M., Rogers, B. M., Randerson, J. T. and Hess, P. G.:
774 The changing radiative forcing of fires: global model estimates for past, present and future,
775 *Atmos. Chem. Phys.*, 12(22), 10857–10886, doi:10.5194/acp-12-10857-2012, 2012.

776 Wotton, B. M., Flannigan, M. D., and Marshall, G. A.: Potential climate change impacts on
777 fire intensity and key wildfire suppression thresholds in Canada, *Environ. Res. Lett.*, 12,
778 095003, <https://doi.org/10.1088/1748-9326/aa7e6e>, 2017.

779 Westerling, A. L., Hidalgo, H. G., Cayan, D. R. and Swetnam, T. W.: Warming and Earlier
780 Spring Increase Western U.S. Forest Wildfire Activity, *Science* (80-.), 313(5789), 940 LP –
781 943, doi:10.1126/science.1128834, 2006.

782 Wotawa, G. and Trainer, M.: The Influence of Canadian Forest Fires on Pollutant
783 Concentrations in the United States, *Science* (80-.), 288(5464), 324 LP – 328,
784 doi:10.1126/science.288.5464.324, 2000.

785 Wu, Y., Arapi, A., Huang, J., Gross, B. and Moshary, F.: Intra-continental wildfire smoke
786 transport and impact on local air quality observed by ground-based and satellite remote
787 sensing in New York City, *Atmos. Environ.*, 187, 266–281,
788 doi:<https://doi.org/10.1016/j.atmosenv.2018.06.006>, 2018.

789 Xue, Z., Gupta, P., and Christopher, S.: Satellite-based estimation of the impacts of
790 summertime wildfires on PM_{2.5} concentration in the United States, *Atmos. Chem. Phys.*, 21,
791 11243–11256, <https://doi.org/10.5194/acp-21-11243-2021>, 2021.

792 Yang, P.-L., Y. Zhang, K. Wang, P. Doraiswamy, and S.-H. Cho, 2019, Health Impacts and
793 Cost-Benefit Analyses of Surface O₃ and PM_{2.5} over the U.S. under Future Climate and
794 Emission Scenarios, *Environmental Research*, 178, November 2019, 108687,
795 <https://doi.org/10.1016/j.envres.2019.108687>.

796 Yue, X., Mickley, L. J., Logan, J. A. and Kaplan, J. O.: Ensemble projections of wildfire
797 activity and carbonaceous aerosol concentrations over the western United States in the mid-
798 21st century, *Atmos. Environ.*, 77, 767–780,
799 doi:<https://doi.org/10.1016/j.atmosenv.2013.06.003>, 2013.

800 Zou, Y., Wang, Y., Ke, Z., Tian, H., Yang, J. and Liu, Y.: Development of a REgion-Specific
801 Ecosystem Feedback Fire (RESFire) Model in the Community Earth System Model, *J. Adv.
802 Model. Earth Syst.*, 11(2), 417–445, doi:10.1029/2018MS001368, 2019.

803 Zou, Y., Wang, Y., Qian, Y., Tian, H., Yang, J. and Alvarado, E.: Using CESM-RESFire to
804 understand climate–fire–ecosystem interactions and the implications for decadal climate
805 variability, *Atmos. Chem. Phys.*, 20, 995–1020, <https://doi.org/10.5194/acp-20-995-2020>,
806 2020.

807 Zhang, Y., P.-L. Yang, Y. Gao, R. L. Leung, and M. Bell, 2020, Health and Economic
808 Impacts of Air Pollution Induced by Climate Extremes over the Continental U.S.,
809 *Environmental International*, 143, 105921, <https://doi.org/10.1016/j.envint.2020.105921>.

810

811